Charge to Mass

Yunran Yang
Jacqueline Zhu

1 Abstract

This lab investigates the charge-to-mass (e/m) of the electron by analyzing its circular motion subjected to a uniform magnetic field produced by Helmholtz coils. The total magnetic field acting on the electrons were corrected for background magnetic effects, and uncertainties were propagated through experimental measurements. The two experimental setups yield values of $(1.21 \pm 0.15 \times 10^{11}$C/kg and $(1.93 \pm 0.04 \times 10^{11}$C/kg with percentage errors of 31.3% and 9.66%, respectively. The discrepancy is mainly due to variations in external magnetic influences, along with other errors discussed later.

2 Introduction

The charge-to-mass ratio $\frac{e}{m}$ of the electron is a fundamental physical constant that characterizes the behavior of electrons in electromagnetic fields. In this experiment, $\frac{e}{m}$ is determined by analyzing the circular motion of electrons subjected to a uniform magnetic field generated by Helmholtz coils.

The total magnetic field B acting on the electron beam includes both the controllable field from the Helmholtz coils, B_c, and the background external magnetic field, B_e:

$$B = B_c + B_e \tag{1}$$

The magnetic field from the Helmholtz coils is given by:

$$B_c = \left(\frac{4}{5}\right)^{\frac{3}{2}} \frac{\mu_0 \, n \, I}{R} \tag{2}$$

where μ_0 is the permeability of free space, n =130 is the number of turns in the coils, I is the current through the coils, and R=0.15m is the radius of the coils.

Because the magnetic field is not completely uniform, a correction must be applied to account for the radial displacement ρ of the electron beam from the central axis. This correction modifies the magnetic field according to:

$$\frac{B_c(\rho)}{B_c(0)} = 1 - \frac{\rho^4}{R^4 \left(0.6583 + 0.29\frac{\rho^2}{R^2}\right)^2} \tag{3}$$

The radius of the electron beam's circular trajectory is related to the applied voltage ΔV, the magnetic field, and the charge-to-mass ratio. Rearranging Newton's second law and the Lorentz force law gives the curvature of the path as:

$$\frac{\sqrt{\Delta V}}{r} = \sqrt{\frac{e}{m}} \, k(I + \tfrac{1}{\sqrt{2}} \, I_0 \,) \tag{4}$$

where $k = \frac{1}{\sqrt{2}} \left(\frac{4}{5}\right)^{\frac{3}{2}} \frac{\mu_0 \, n}{R}$ is a constant determined by the geometry of the coils, and $I_0 = \frac{B_e}{k}$ represents the effective current equivalent of the background magnetic field.

To isolate B_e, the corrected magnetic field B_c is plotted against the inverse radius $\frac{1}{r}$. The resulting linear relationship follows:

$$B_c = \alpha \frac{1}{r} + B_e \tag{5}$$

Here, α is the slope of the fit and $\alpha = \sqrt{\frac{2m}{e}\Delta V}$

3 Methodology

3.1 Materials

1. Anode voltage meter (MM1)
2. Coil current meter (MM2)
3. Electron gun (EG)
4. Glass bulb (GB)
5. Helmholtz coil (HC)
6. Power bus (PB)
7. Rheostat (R)
8. Self-illuminated scale
9. Plastic reflector
10. Banana wires

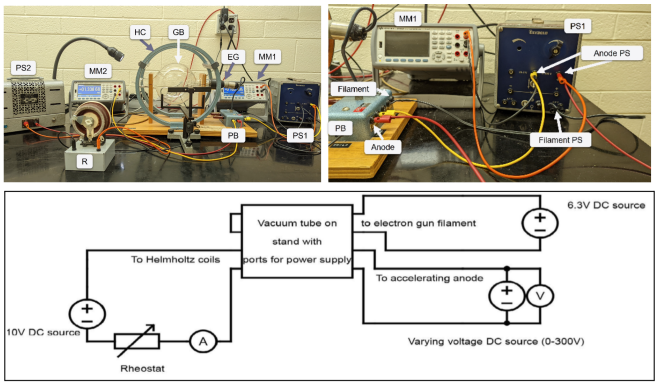

Figure 1: Photo of experimental setup and diagram of the circuit [1]

3.2 Methods

1. The apparatus was assembled based on the diagram in Figure 1. The power supply for the electron gun filament (Filament PS) was turned on for 30 seconds to heat up the filament.
2. The anode voltage and Helmholtz coil power supply (Anode PS and PS1) were activated. Once the electrons gained enough kinetic energy, the beam became visible inside the glass bulb.
3. A self-illuminated scale and plastic reflector were positioned with the reflector placed between the scale and the glass bulb. The base of the scale was aligned parallel to the base of the glass bulb (GB). The rightmost measurement mark of the scale was aligned with the rightmost point of the electron beam's trajectory.
4. A self-illuminated scale was used instead of a rule to: (1) minimize parallax error, which will be discussed later in section 5.1; (2) improve visibility and alignment due to its lighting.
5. To measure the diameters of the electron beam's trajectory, the two conditions below were applied. For both conditions, three sets of data were recorded. As we vary the constants, the glass bulb was rotated as necessary to ensure that the electron beam remained in a closed loop.
   (a) Constant current, varying voltage: current was maintained at 1.267 A. Anode voltage was adjusted from 150.09 V to 350.01 V using the power supply knobs.
   (b) Constant voltage, varying current: anode voltage was fixed at 250.082 V. current was varied from 1.120 A to 1.921 A using the rheostat (Figure 1).

4 Data and Analysis

4.1 Magnetic Field

The uncorrected magnetic field is initially determined using Equation 3 based on the measured coil current. However, the magnetic field produced by the Helmholtz coils is not perfectly uniform, meaning the electrons experience variations in the field strength as they move away from the central axis. To account

for this, a correction must be applied that considers the electron trajectory's radius, ρ, to have a more accurate representation of the field influencing the electrons. For each data set, the trajectory radius is estimated using the measured beam radius. The corrected magnetic field $B_c(\rho)$ is obtained by applying this factor to $B_c(0)$. Complete results from this calculation can be found in Appendix 4.

4.2 External Magnetic Field B_e

Two complementary measurements were conducted. In the first set, the coil current I was held constant ($I = 1.267$ A) while the accelerating voltage ΔV was varied. In the second set, ΔV was kept constant ($\Delta V = 250$ V) while I was varied. To determine the external magnetic field B_e, only the second dataset is used according to Equation 5, since the slope of the linear fit depends on constant accelerating voltage ΔV, and constant current results in constant B_c.

The magnetic field generated by the coils, B_c, is calculated using Equation 2 and corrected by a factor of $B_c(\rho)/B_c(0)$. Given that the number of coil turns n is a defined integer and the coil radius R is provided as a fixed constant, both are assumed to have negligible uncertainty. Since each measurement of I was repeated three times, the uncertainty in the mean current was estimated using the standard error:

$$\sigma_{\bar{x}} = \frac{\sigma_x}{\sqrt{n}}$$

with

$$\sigma_x = \sqrt{\frac{\sum(x_i - \bar{x})^2}{n-1}}$$

where x_i are the individual measurements, $\bar{x}$ is their mean, and n is the number of trials. Defining the prefactor as $\kappa = \left(\frac{4}{5}\right)^{3/2} \frac{\mu_0 n}{R}$. Let $\left(\frac{4}{5}\right)^{3/2} \frac{\mu_0 n}{R} = \kappa$, it can be determined that

$$\Delta B_c = \kappa \Delta I = \kappa \sigma_{\bar{x}}$$

The uncertainty in the curvature of electron orbit, $\frac{1}{r}$, is found to be $\Delta(\frac{1}{r}) = \frac{\Delta r}{r^2}$, given Δr is the uncertainty of the self-illuminated scale and has a value of 0.0005 m.

The results are illustrated in the following figures, and the lines of best fit are evaluated by residual plots, R^2 and reduced chi-squared χ^2_ν (calculation see Appendix 5.4) :

Set 2 measurements yield the following linear relationship between the corrected magnetic field B_c and the inverse beam radius $1/r$:

$$B_c = (5.091 \pm 0.061) \times 10^{-5} \cdot \frac{1}{r} - (1.02 \pm 1.43) \times 10^{-5}.$$

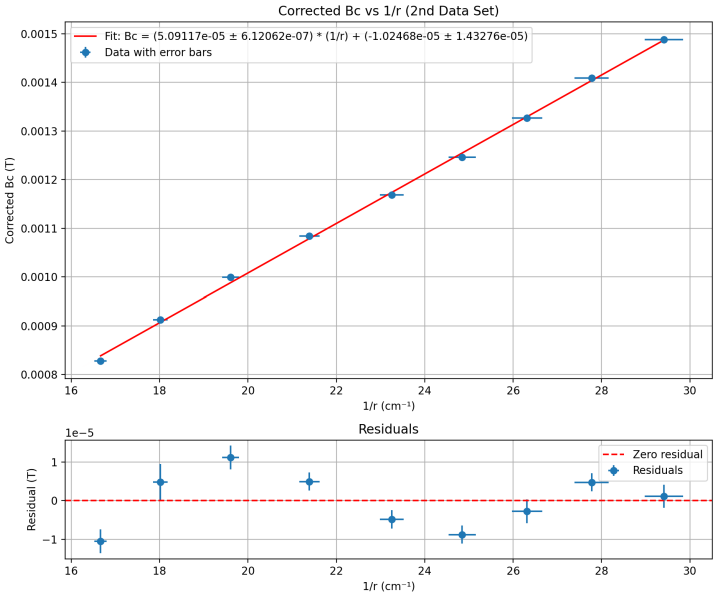

Figure 2: Set 2: Accelerating voltage ΔV held constant while coil current I is varied. The corrected magnetic field B_c is plotted against inverse beam radius $1/r$. Error bars for B_c are present but not visible due to their small magnitude. The best-fit line gives $R^2 = 0.996$ and a randomly scattered residual plot, again indicating strong linearity, but a reduced chi-squared value of $\chi^2_\nu = 0.565$ suggests overfitting.

Quantity	Set 1	Set 2
α (T m)	/	$(5.091 \pm 0.061) \times 10^{-5}$
B_e (T)	/	$(1.02 \pm 1.43) \times 10^{-5}$

Table 1: Comparison of the linear-fit slope α and the extra field B_e for the two data sets.

4.3 Charge to Mass Ratio

By rearranging Equation 5, charge to mass ratio e/m can be expressed as:

$$\frac{e}{m} = \frac{2\,\Delta V}{\alpha^2} \tag{6}$$

when accelerating voltage ΔV is constant (uncertainty calculation see Appendix 5.4).

In contrast, for the first set of measurements where ΔV is fixed and I is varied, a linear relationship between $\frac{1}{r}$ and $(I + \frac{1}{\sqrt{2}} I_0)/\sqrt{\Delta V}$ can be established according to Equation 4. The slope α of the linear fit corresponds to $\sqrt{\frac{e}{m}}\, k$, from which the charge-to-mass ratio can be calculated as (error propagation see Appendix 5.4):

$$\frac{e}{m} = \left(\frac{\alpha}{k}\right)^2$$

Using the estimation of $B_e \approx 0$ from the previous section, it's found $I_0 = B_e/k \approx 0$. The best line of fit yields in linear relation:

$$\frac{1}{r} = (1.911 \pm 0.065) \times 10^2 \cdot \frac{I}{\sqrt{V}} + (-5.78 \pm 0.54)$$

According to the results obtained in the previous section, the experimental charge-to-mass ratio values for both sets can be obtained:

Set	e/m (C/kg)	% Error
Set 1	$(1.21 \pm 0.15) \times 10^{11}$	31.3%
Set 2	$(1.93 \pm 0.04) \times 10^{11}$	9.66%

Table 2: Calculated e/m for both sets. The accepted value is approximately 1.76×10^{11} C/kg.

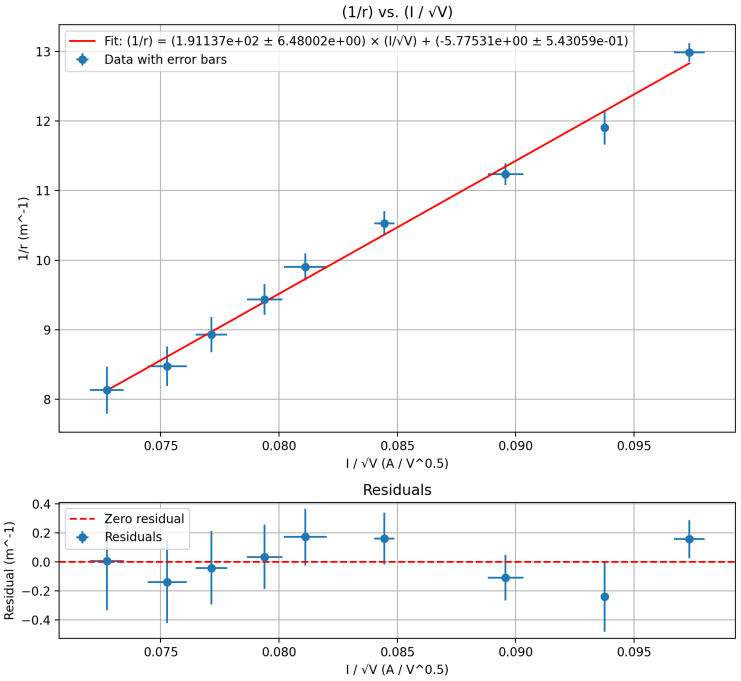

Figure 3: Set 1: Coil current I held constant while accelerating voltage ΔV is varied. The plot shows the linear relationship between corrected magnetic field B_c (including the off-axis correction factor) and inverse radius $1/r$. The best-fit line yields $R^2 = 0.994$, indicating a strong linear trend. The residual plot shows randomly scattered points above and below the zero line, further supporting a good fit. However, the reduced chi-squared value $\chi^2_\nu = 0.469$ suggests that the uncertainties may be overestimated or that systematic deviations from the model exist.

5 Discussion and Conclusion

5.1 Parallax Effect

Parallax errors occur when the observer is not perfectly aligned with the measurement scale. The self-illuminated scale makes itself visible to allow the observer to clearly see the markings without shadows or reflections. This bright display minimizes errors in misalignment. The plastic reflector allows the observer to view the reflection of the scale with the beam, so it can be adjusted until the two images coincide. This method with the use of a self-illuminated scale can reduce systematic measurement errors.

5.2 Electron Trajectory

When the accelerating voltage is low, the electrons gain less kinetic energy, which results in a lower velocity. At the same time, a high coil current generates a strong magnetic field, which increases the Lorentz force. A lower velocity and a stronger field will lead to a much smaller trajectory radius of curvature.

Not all parts of the trajectory are equally affected: (1) The Helmholtz has a nearly uniform field at the center, but the strong magnetic field exaggerates edge effects, which distorts the uniform circuit path. (2) At low velocities, electronics have a wider range of initial velocities from temperature differences. (3) Since the experiment occurs in a low-pressure environment, electronics are more susceptible to scattering from residual gas molecules. (4) In strong magnetic fields, electronics moving parallel to field lines experience a force pushing them back. This introduces errors in the measurement of electron trajectory due to non-circular trajectories, scattering of electron beams, and misalignment of field lines. To reduce the errors, we can raise the accelerating voltage to increase velocity, lower the magnetic field to reduce current in order to have a more defined circular trajectory.

5.3 Extra Magnetic Field B_e

As observed from the previous section, two scenarios arise from varying either the coil current or the accelerating voltage. In the case of low, fixed coil current and increasing accelerating voltage, the magnetic field remains effectively constant. As ΔV increase, the electrons gain higher speed, causing the radius of the orbit to increase according to Equation 4. Additionally, higher-energy electrons excite the residual gas atoms inside the glass bulb more effectively, producing more visible light per collision. Thus the electron trajectory appear slightly brighter as the accelerating voltage increases. Conversely, when ΔV is fixed and relatively high, but the coil current is raised, the magnetic field grows stronger and forces the electrons onto a tighter circular path. Since the electron energy remains constant in this case, the brightness per collision does not change, consistent with the observation.

The measured extra magnetic field B_e was found to be $(1.02 \pm 1.43) \times 10^{-5}\,\mathrm{T}$ for Set 2 measurements. This value is smaller than the average magnetic field at Earth's surface, $B_{\text{earth}} \approx 5 \times 10^{-5}\,\mathrm{T}$. Notably, the uncertainty (1.43×10^{-5}) is greater than the measured value, indicating that the result is statistically consistent with $B_e = 0$ within experimental error. This suggests that no significant external magnetic field was detected in the experimental region.

This outcome is reasonable since Helmholtz coils are designed to produce a uniform magnetic field and can be oriented to partially or fully cancel external external magnetic fields such as Earth's magnetic field along the coil axis [2]. However, when a phone was placed near the glass bulb, a visible alteration of the electron beam trajectory was observed and B_e was found to increase. The closer the phone (which contains magnetic materials and electronic components) was to the setup, the more pronounced the deflection. This suggests the presence of additional magnetic influences within the laboratory environment. The near-zero value of B_e may therefore be a result of magnetic field compensation. Nearby ferromagnetic objects or devices such as power supplies and electronics can distort or counteract the Earth's magnetic field at the apparatus location. These local sources likely contribute to the uncertainty in the measurements. Conducting the experiment in an environment free from unnecessary magnetic materials, or using magnetic shielding, would help reduce extraneous fields and improve the accuracy of the measured values.

5.4 Charge to Mass Ratio

The two sets of experiments yield in experimental e/m of $(1.21 \pm 0.15) \times 10^{11} C/Kg$ (%error = 31.3%) and$(1.93 \pm 0.04) \times 10^{11}$ (%error = 9.66%) respectively. Although both sets used the same apparatus, the result from Set 1 exhibits a significantly larger percentage error. One likely explanation is that the Set 1 analysis employed a value for the external field, B_e, that was determined from Set 2 measurement. Even with efforts to keep electronic devices and ferromagnetic materials far from the Helmholtz coil region, slight changes in local magnetic environments can influence the beam radius measurements differently across the two data runs.

These findings suggest that while the underlying physical relationship between electron velocity, magnetic field strength, and beam radius is validated, each dataset remains susceptible to systematic uncertainties such as slight misalignments, unaccounted local fields, and instrumental limits in voltage and current precision. Nonetheless, the values obtained fall within a comparable range of the accepted theoretical charge-to-mass ratio, demonstrating that the experimental procedure and apparatus reliably capture the essential physics of electron motion in a magnetic field despite the aforementioned sources of error.

References

[1] H. Zhan, E. Horsley, and A. Harlick, *Charge-to-Mass Ratio for the Electron*, University of Toronto, Physics Department, rev. 3fcb776, Mar. 17, 2025. [Online]. Available: http://creativecommons.org/licenses/by-nc-sa/4.0/

[2] Wikipedia contributors, "Helmholtz coil," *Wikipedia, The Free Encyclopedia*, Apr. 1, 2025. [Online]. Available: https://en.wikipedia.org/wiki/Helmholtz_coil

Appendix

Reduced Chi-squared

The reduced chi-squared value was calculated using equation

$$\chi^2_\nu = \frac{\chi^2}{v}, \text{where } \chi^2 = \sum_{i=1}^{N} \frac{[y_i - f(x_i)]^2}{\sigma^2_{y_i}}$$

and v is the degree of freedom.

e/m Uncertainty Derivation

Set 1: Constant I, varying ΔV

$$\Delta\left(\frac{e}{m}\right) = \frac{1}{k^2 r^2} \cdot \sqrt{\left(\frac{1}{2A^2\sqrt{\Delta V}} \cdot \Delta(\Delta V)\right)^2 + \left(\frac{2\sqrt{\Delta V}}{A^3} \cdot \Delta I\right)^2 + \left(\frac{2\sqrt{\Delta V}}{A^3} \cdot \frac{1}{\sqrt{2}} \cdot \Delta I_0\right)^2}$$

Set 2: Constant ΔV, varying I

The total uncertainty is then derived using error propagation:

$$\begin{aligned}\Delta(\frac{e}{m}) &= \sqrt{(\frac{\partial f}{\partial V}\Delta V)^2 + (\frac{\partial f}{\partial \alpha}\Delta\alpha)^2} \\ &= \frac{2}{\alpha^2}\sqrt{(\Delta V)^2 + 4(\frac{V^2}{\alpha^2})(\Delta\alpha)^2}\end{aligned}$$

Current (A)	Voltage (V)	Diameter (cm)	Radius (cm)	rho/R	Correction Facto	CF_uncertainty	B_c	Bc_uncertainty	Corrected_Bc	CB_uncertainty
1.267	150.09	7.7	3.850	0.257	0.991	0.000429	9.8736E-04	2.36E-06	9.7802E-04	2.36E-06
1.267	175.09	8.4	4.200	0.280	0.987	0.000395	9.8736E-04	1.56E-06	9.7427E-04	1.56E-06
1.267	200.09	8.9	4.450	0.297	0.983	0.000373	9.8736E-04	1.55E-06	9.7100E-04	1.55E-06
1.267	225.09	9.5	4.750	0.317	0.979	0.000283	9.8736E-04	2.34E-06	9.6634E-04	2.34E-06
1.267	250.08	10.1	5.050	0.337	0.973	0.000251	9.8736E-04	3.12E-06	9.6080E-04	3.12E-06
1.267	275.07	10.6	5.300	0.353	0.968	0.000185	9.8736E-04	2.34E-06	9.5545E-04	2.34E-06
1.267	300.06	11.2	5.600	0.373	0.960	0.000124	9.8736E-04	1.56E-06	9.4807E-04	1.56E-06
1.267	325.02	11.8	5.900	0.393	0.952	0.000102	9.8736E-04	2.34E-06	9.3956E-04	2.34E-06
1.267	350.01	12.3	6.150	0.410	0.943	0.000091	9.8736E-04	2.34E-06	9.3155E-04	2.34E-06

voltage (V)	current (A)	Diameter (cm)	Radius (cm)	rho/R	Correction Facto	CF_uncertainty	B_c	Bc_uncertainty	Corrected_Bc	CB_uncertainty
250.082	1.12	12	6.000	0.400	0.948	0.000653	8.7280E-04	3.12E-06	8.2781E-04	3.12E-06
250.082	1.217	11.1	5.550	0.370	0.962	0.000639	9.4839E-04	4.67E-06	9.1191E-04	4.67E-06
250.082	1.319	10.2	5.100	0.340	0.972	0.000578	1.0279E-03	3.10E-06	9.9918E-04	3.10E-06
250.082	1.419	9.35	4.675	0.312	0.980	0.000543	1.1058E-03	2.34E-06	1.0837E-03	2.34E-06
250.082	1.522	8.6	4.300	0.287	0.985	0.000462	1.1861E-03	2.36E-06	1.1689E-03	2.36E-06
250.082	1.617	8.05	4.025	0.268	0.989	0.000246	1.2601E-03	2.31E-06	1.2459E-03	2.31E-06
250.082	1.718	7.6	3.800	0.253	0.991	0.000219	1.3388E-03	3.12E-06	1.3268E-03	3.12E-06
250.082	1.821	7.2	3.600	0.240	0.993	0.000192	1.4191E-03	2.34E-06	1.4087E-03	2.34E-06
250.082	1.921	6.8	3.400	0.227	0.994	0.000125	1.4970E-03	2.98E-06	1.4883E-03	2.98E-06

Figure 4: Table of raw and calculated data for voltage, current, $B_c(0)$, ρ, and $B_c(p)$ with their respective uncertainties.